Morphological, ultrastructural, and biochemical changes induced by sodium fluoride in the tongue of adult male albino rat and the ameliorative effect of resveratrol

Emtethal M. El-Bestawy, Asmaa M. Tolba, Walaa A. Rashad

Department of Human Anatomy and Embryology, Faculty of Medicine, Zagazig University, Sharqia Governorate, Egypt

Abstract: Little knowledge is available about the effects of fluoride exposure on the tongue. This study evaluated the effects of sodium fluoride (NaF) on the tongue ultrastructure and detected the ameliorative effects of resveratrol. Forty adult albino rats were separated into 4 groups: the control group was given a balanced diet and purified water. The NaF treated group: received 10 mg/kg/d dissolved in 2.5 ml distilled water once daily for 30 days orally. The NaF+resveratrol group: received NaF 10 mg/kg/d orally together with resveratrol in a dose of 30 mg/kg daily for 30 days. The resveratrol group was subjected to resveratrol in a dose of 30 mg/kg/d by oral gavage for 30 days. Sections were stained with hematoxylin & eosin, and Masson's trichrome. Tumor necrosis factor α immunohistochemical study and electron microscopic examinations were done. The oxidative stress markers malondialdehyde, antioxidant reduced glutathione, and the total antioxidant capacity were measured. The NaF group revealed ulceration, necrotic muscle fibers, distorted papillae and a significant increase in malondialdehyde level, and a significant decrease in glutathione and the total antioxidant levels. In the NaF+resveratrol group, pathological changes were less, and the oxidant levels were decreased by the administration of resveratrol with NaF. In conclusion, NaF adversely affects the ultrastructure of the adult rat tongue and resveratrol can ameliorate this effect.

Key words: Sodium flouride, Resveratrol, Tongue, Rat, Electron microscopy

Introduction

Fluoride is widely distributed in nature at high concentrations [1]. It is a natural element in the crust of the earth and presents in different concentrations in air, water, soil, and rocks. Sodium fluoride (NaF) is considered to be a life-supporting trace element from the halogen group [2, 3].

NaF is a protective agent against dental cavities and plays a role in the normal mineralization of bone [4]. American communities added fluoride to tap water to decrease dental caries since 1940. Then, many countries added it to drinking water for clarification purposes. Dark green vegetables are regarded as a main source of fluoride, it accumulates in their leaf as it is obtained from the water and soil [5]. Many people are exposed to fluoride in an acute or chronic ways [6]. A variable amount of fluoride exists in colas, sports drinks, beers, carbonated soft drinks, and reconstituted juices, and in the chemical organic or inorganic forms; one of the most commonest inorganic fluorides is the sodium [7]. NaF is commonly used in the fluorination of drinking water. Moreover, it is commonly used as a fungicide pesticide, ro-

Corresponding author:
Asmaa M. Tolba [ORCID]
Department of Human Anatomy and Embryology, Faculty of Medicine, Zagazig University, Sharqia Governorate 44519, Egypt
E-mail: asmaaabdalaal1980@gmail.com

denticide, and a component in glass and dental laboratories [8]. Via topical application in the mouth rinse and kinds of dental toothpaste, NaF can prevent caries. It is also present in infant formulas, processed cereals, and canned fish [9]. Like many elements, fluoride is beneficial to human health in trace amounts but can be toxic in excess [10]. Excessive daily intake for a long period may result in fluorosis which is a serious public health problem [11]. Dental and skeletal fluorosis was reported to be the early toxic effects of fluoride in humans especially in areas with an elevated exposure to it. Besides, its excessive accumulation in the body can exert toxic effects on many tissues and organs resulting in severe symptoms and pathological changes [12]. Fluoride is absorbed completely and quickly from the gastrointestinal tract and crosses the cell membranes to enter the soft tissues resulting in impairment of their functions [13]. Moreover, fluoride can pass through the blood brain barrier and cause adverse effects on mental functions [14, 15]. After chronic fluoride administration, aberrant behavior patterns, altered neuronal and cerebrovascular integrity and metabolic abnormalities were found in the animals' blood, brain, and liver [16]. The harmful effects of fluoride are influenced by the production of free radicals, lipid peroxidation, and alterations in the antioxidant defense mechanisms [17]. Tongue ulcers are common pathological disorders, the mechanism of the oral ulcer formation includes cytokine production, blood flow decrease, and cell death [18]. Tongue ulcer treatment is so important, therefore, many medical therapies for tongue ulcers have been developed [19]. Medicinal plants are used as complementary medicine all over the world because of their potential health benefits. For therapeutic purposes, many plant extracts can be used with fewer possible complications [20]. Resveratrol is a polyphenolic molecule (trans-3, 4', 5-trihydroxystilbene) that can be found in a variety of plants, including grapes, herbs, peanuts, and berries [21]. Resveratrol is a natural antioxidant that regulates cellular protection against oxidative stress in many diseases, including cardiovascular, neurodegeneration, aging, diabetes, and cancer [22]. However, whether resveratrol can attenuate the NaF toxicity on the tongue has not been reported. Although there are many studies on the relationship between the NaF and the oxidative stress, very limited systematic studies are focused on the pathological changes in the tongue through the NaF oxidative stress. In this study, the NaF induced oxidative damage was evaluated through the ultrastructure examination of the tongue and the possible protective effects of resveratrol were determined by immunohistochemical estimation of the inflammatory marker tumor necrosis factor α (TNF-α).

Materials and Methods

Chemicals

NaF: In powder form. The purity is >98%. Resveratrol, malondialdehyde (MDA), and reduced glutathione (GSH) were obtained from Sigma Chemical Co. (St. Louis, MO, USA).

Animals

In this study, 40 adult male Wistar albino rats weighing 220 to 250 g aged about 3 to 4 months were obtained from the Zagazig Scientific Medical Research Center. They were kept in a pathogen-free environment in large polypropylene animal cages in the prevailing ambient conditions at room temperature; ranging between 18°C and 22°C. Their diet consisted of a well-balanced meal of ordinary chow. Rats were acclimatized to the experimental conditions for 2 weeks before the experiment. All experimental procedures were carried out in conformity with the appropriate standards and regulatory guidelines of the Zagazig Institutional Animal Care and Use Committee (approval no. ZU-IACUC/3/F/209/2021).

Experimental design

Rats were separated into four groups each contained ten rats (n=10):

Control group (Group I): animals were given a balanced diet and purified water for 30 days.

NaF-treated group (Group II): rats were subjected to 10 mg/kg/d NaF by oral gavage for 30 days [23].

NaF+resveratrol group (Group III): rats received NaF 10 mg/kg/d by oral gavage together with resveratrol in a dose of 30 mg/kg daily for 30 days.

Resveratrol group (Group IV): rats were subjected to resveratrol in a dose of 30 mg/kg daily by oral gavage for 30 days [24].

At the end of the experimental period, the rats were sedated with sodium thiopental intraperitoneally to apply the experimental procedures and their tongues were removed for further procedures to be applied:

Tongue weight assessment

The removed rat tongues were weighed by using digital scale.

Gross morphology assessment

The tongue was carefully examined by naked eyes for changes in shape, color, size, and consistency. The gross morphological changes were photographed by 13+5 megapixel dual rear camera of Samsung galaxy A20 phone (Samsung, Seoul, Korea).

Histological technique

Light microscopic study

The tongue was immediately soaked in 10% buffered formalin before being processed and embedded in paraffin wax as per the standard procedure. Hematoxylin & eosin (H&E) and Masson's trichrome (MT) were used to stain 5-μm thick sections [25].

Immunohistochemical examination

Immunohistochemical examinations were carried out based on the streptavidin-biotin immune-peroxidase technique. Four-μm paraffin sections were mounted, dewaxed, and rehydrated with phosphate buffered saline (PBS) (pH 7.2). Then, heat induced antigen retrieval was undertaken in citrate buffer (pH 6) for 20 minutes. In order to block the activity of endogenous peroxidase, sections were treated with 3% hydrogen peroxide for 10 minutes and washed in PBS. Overnight incubation of slides with the primary antibody anti TNF-α rabbit polyclonal antibody (1:50 dilution, Cat. No. A0277; AB clonal, Woburn, MA, USA) was undertaken. Then, slides were incubated with a secondary antibody and visualized by using the chromagen (3, 3'-diaminobenzidine tetrahydrochloride). Sections were counterstained with Mayer's hematoxylin, washed with distilled water and PBS, dehydrated, and mounted. Light microscopic examination was done at the Department of Anatomy, Faculty of Medicine, Zagazig University. The images of the histological sections were obtained using a light microscope fitted with a digital camera (The Leica DM500 microscope, Leica ICC50 W Camera Modul, Cambridge, UK, Anatomy Department, Faculty of Medicine, Zagazig University, Egypt).

Ultrastructural study

Scanning electron microscopic examination

After fixation of the tongue specimens in 4% phosphate-buffered glutaraldehyde (0.1 mol/L, pH 7.4), they were post-fixed in 1% phosphate-buffered osmium tetroxide. Then the specimens were dehydrated in serial dilutions of ethanol and placed into amyl acetate. The samples were then dried with liquid CO^2 and coated with gold particles [26]. The tongue sample mounting was performed on aluminum stubs and scanning examination was done under scanning electron microscopic examination (JEOL JSM-6510 LV electron microscope; Jeol Ltd, Tokyo, Japan; Faculty of Agriculture, Electron Microscope Research Unit, Al-Mansoura University, Egypt).

Transmission electron microscopic examination

The tongue tissue specimens were cut into about 1 mm^3 section and fixed in 2.5 percent phosphate-buffered glutaraldehyde in 0.1 sodium phosphate buffer (pH 7.2). After that, post fixation of the samples was done in 1% osmium tetroxide, followed by washing in distilled water, then dehydration in a succession of graded alcohols, and finally acetone. In a final step, the samples were encased in epoxy resin and left overnight at 60°C for polymerization. Semithin sections,1-μm thick, were cut by ultra-microtome and stained with 1% toluidine blue for light microscopic examination. After polymerization, 80 to 90 nm ultrathin sections were stained with 5% uranyl acetate for 15 minutes and 8% lead citrate for 8 minutes [27]. Examination and photographing of the specimens were done by transmission electron microscope (JEOL JEM-2100; Tokyo, Japan, Faculty of Agriculture, Electron Microscope Research Unit, Al-Mansoura University, Egypt).

Biochemical analysis

Determination of the oxidative stress and antioxidant markers MDA in nmol/g, GSH in mg/g, and the total antioxidant capacity in mmol/l were measured in the tongue homogenate using their relevant kits. The tongue was homogenized (1:10 w/v) in phosphate-buffered saline (100 mM) containing ethylenediaminetetraacetic acid (1 mM, pH 7.4) and centrifuged (12,000×g, 30 minutes, 4°C). The resulting supernatant was separated and kept at –80°C for biochemical analysis [28].
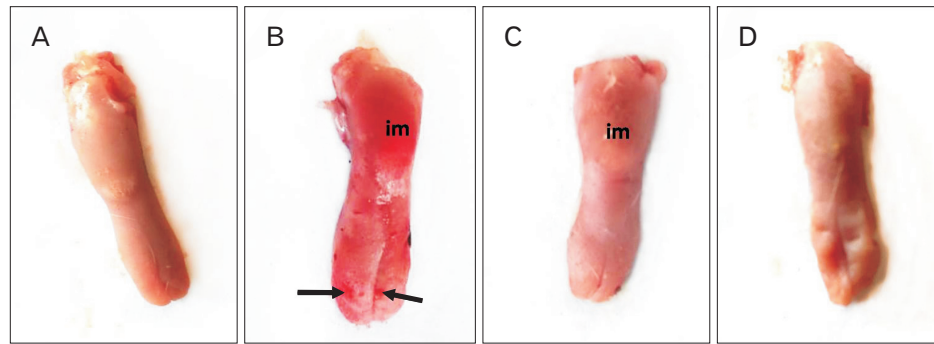
Fig. 1. A photomicrograph shows the gross morphological changes of the albino rat tongue induced by sodium fluoride and their amelioration by resveratrol. (A) Control group shows a normal appearance of the rat tongue. (B) NaF treated group, displays a red tongue with marked congestion of the dorsal surface over the intermolar prominence (im) and ulcers (arrows) on the anterior part of the dorsal surface. (C) NaF+resveratrol group shows marked improvement but still shows some congestion in the posterior part of the dorsal surface over the intermolar prominence (im). (D) Resveratrol group exhibits a normal appearance of the rat tongue which looks like the control group. NaF, sodium fluoride.

Morphometrical analysis

Using ImageJ analysis software (National Institutes of Health, Bethesda, MD, USA), the area percentage (AP) of the collagen fibers and the optical density (OD) of TNF-α immune expression were calculated.

Statistical analysis

SPSS software (ver. 19.0; IBM Corp., Armonk, NY, USA) was used for the statistical analysis of the collected data and a mean±standard deviation was used to represent the data. Analysis of variance (ANOVA) and the least significant difference (LSD) *post-hoc* test were used to examine the data. A P-values of less than 0.05 were considered significant.

Results

Gross morphological assessment

In the current study, the tongue of the control and the resveratrol groups showed the normal gross morphological appearance of the dorsal surface with regular size and shape (Fig. 1A, D). While the dorsal surface of the tongue of the NaF treated group appeared red with marked congestion over the intermolar prominence and ulcers were produced on the anterior segment of the dorsal surface of the tongue (Fig. 1B). The NaF+resveratrol group showed markedly improved tongue appearance in comparison to the NaF treated group, but there was some congestion still present in the posterior part of the dorsal surface of the tongue over the intermolar prominence (Fig. 1C).

Histological results

Light microscopic examination

Hematoxylin & eosin stained sections

In the present study, tongue sections of the control group revealed normal long pointed filiform papillae with overlaying keratinized layer and underlying connective tissue layer of the lamina propria. The fungiform papillae appeared mushroom shaped with centrally situated taste buds. In the muscle layer, fibers were arranged in different directions with vesicular nuclei. Serous and mucous lingual glands were seen (Fig. 2A–D). In the NaF treated group, the filiform papillae appeared atrophied and short. In some sections, the filiform papillae revealed a flattened end. Inflammatory aggregations were observed in the lamina propria and the muscle layer. The fungiform papillae appeared distorted with degenerated taste buds and several vacuolations. The muscle layer showed necrotic areas with a substance loss, the necrotic muscle fibers appeared darkly stained with pyknotic nuclei. Also, separation and fragmentation of the muscle fibers were seen. The congested blood and lymphatic capillaries were observed between the muscle fibers (Fig. 2E–H).

In the NaF+resveratrol group, the filiform papillae appeared less atrophied and some papillae still with flattened end were seen. The fungiform papillae were less deformed with normal centrally situated taste buds. The muscle fibers showed marked preservation of the normal structure but still with necrotic areas with a substance loss and some necrotic darkly stained and fragmented muscle fibers. Adipose tissue was seen between the muscle fibers (Fig. 2I–L). The resvera-
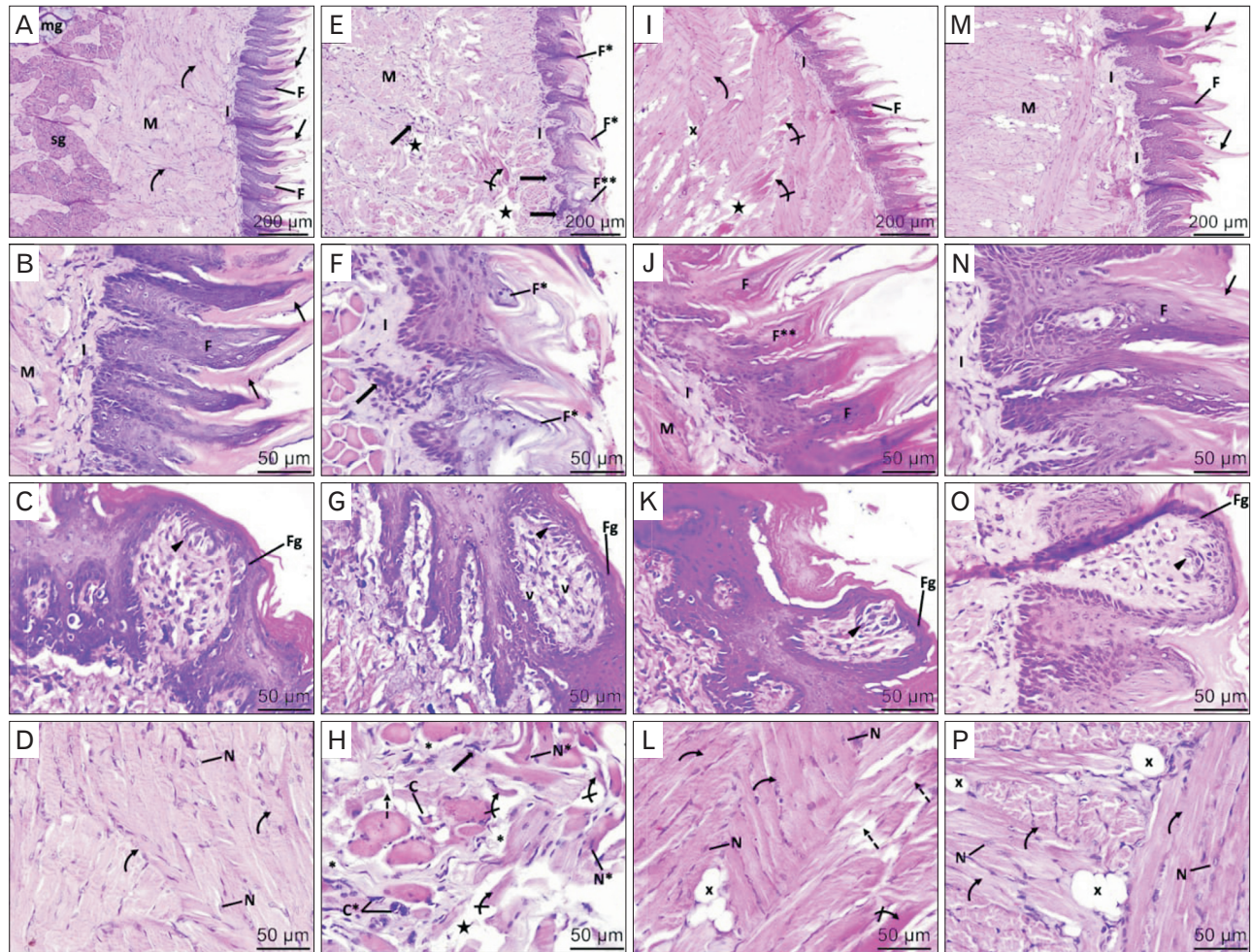
Fig. 2. H&E-stained sections show the pathological changes of the albino rat tongue induced by sodium fluoride and their amelioration by resveratrol. The control group (A–D): (A, B) Long pointed filiform papillae (F) with overlaying keratinized layer (arrows), lamina propria (l), the muscle layer fibers (M) arranged in the different directions (curved arrows), serous (sg) and mucous (mg) lingual glands. (C) Mushroom-shaped fungiform papilla (Fg) with centrally situated taste bud (arrowhead). (D) Muscle fibers are arranged in the different directions (curved arrows) with vesicular nuclei (N). The NaF treated group (E–H): (E, F) Atrophied and short filiform papilla (F*) with a flattened end (F**), inflammatory aggregations (thick arrow) in the lamina propria (l), and the muscle layer (M). The necrotic muscle fibers (crossed curved arrow) and complete necrotic areas with substance loss (star). (G) Deformed fungiform papillae (Fg) with degenerated taste bud (arrowhead) and several vacuolations (v). (H) Separation (*) and fragmentation of the muscle fibers (dotted arrow), necrotic muscle fibers (crossed curved arrow) with pyknotic nuclei (N*), complete necrotic areas with substance loss (star), congested blood capillaries (c), lymphatic capillaries (c*). NaF+resveratrol group (I–L): (I, J) Filiform papillae (F) are less atrophied, some filiform papillae with a flattened end (F**), keratinized layer (arrow), lamina propria (l), muscle layer (M), normal muscle layer fibers (curved arrow), necrotic muscle fibers (crossed curved arrow), complete necrotic areas with substance loss (star), adipose tissue (x). (K) Less deformed fungiform papilla (Fg) with normal centrally situated taste bud (arrowhead). (L) Normal muscle layer fibers (curved arrow) with vesicular nuclei (N), necrotic muscle fibers (crossed curved arrow), fragmented muscle fibers (dotted arrow), and adipose tissue (x). The resveratrol group (M–P): (M, N) Long pointed filiform papillae (F) with overlaying, lamina propria (l), the muscle layer fibers (M). (O) Mushroom-shaped fungiform papilla (Fg) with centrally situated taste bud (arrowhead). (P) Muscle fibers are arranged in the different directions (curved arrow) with vesicular nuclei (N), and adipose tissue (x). H&E staining; (A, E, I, M) ×100, scale bars=200 μm; (B–D, F, G, J–L, N–P) ×400, scale bars=50 μm.

trol group showed normal structure; long pointed filiform papillae with overlaying keratinized layer and underlying connective tissue layer of the lamina propria. The muscle fibers were arranged in different directions with adipose tissue

was also observed in between them (Fig. 2M–P).

Masson's trichrome stained sections
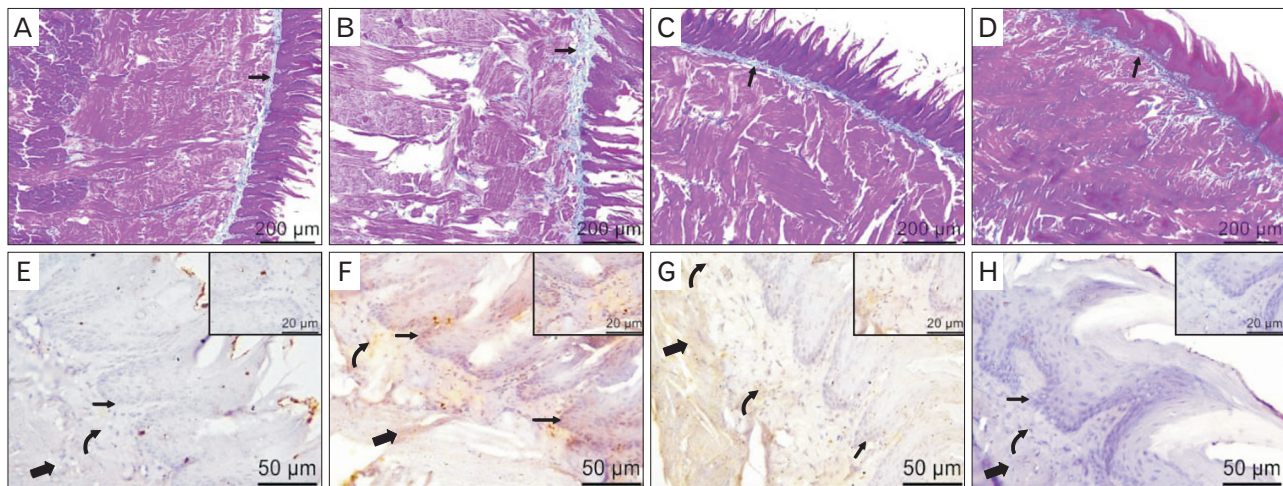MT-stained sections of the control group showed a little

Fig. 3. The albino rat tongue sections reveal the collagen fibers and tumor necrosis factor α (TNF-α) immune expression changes induced by sodium fluoride and their amelioration by resveratrol. (A) Control group shows a little amount of blue-stained collagen fibers (arrow) in the lamina propria. (B) NaF treated group shows an excess amount of blue-stained collagen fibers (arrow) in the lamina propria. (C) NaF+resveratrol group shows a moderate amount of the blue-stained collagen fibers (arrow) in the lamina propria. (D) Resveratrol group shows a little amount of the blue-stained collagen fibers (arrow) in the lamina propria. (E) Control group shows a negative TNF-α immunoreaction in the papillary epithelium (arrow), the lamina propria (curved arrow), and the muscle fibers (thick arrow). (F) NaF treated group displays a strong positive cellular cytoplasmic TNF-α immunoreaction in the papillary epithelium (arrow), the lamina propria (curved arrow), and the muscle fibers (thick arrow). (G) NaF+resveratrol group displays a weak positive cellular cytoplasmic TNF-α immunoreaction in the papillary epithelium (arrow) and a moderate positive immunoreaction in the lamina propria (curved arrow) and the muscle fibers (thick arrow). (H) Resveratrol group exhibits a negative cellular cytoplasmic TNF-α immunoreaction in the papillary epithelium (arrow), the lamina propria (curved arrow), and the muscle fibers (thick arrow). (A–D) Masson's trichrome staining, ×100, scale bars=200 μm; (E–H) TNF-α immunohistochemical staining, ×400, scale bars=50 μm; Inset higher magnification figures: ×1,000, scale bars=20 μm.

amount of the blue collagen fibers distributed in the lamina propria (Fig. 3A). In the NaF treated group, relatively excess collagen in the lamina propria was seen (Fig. 3B). However, a moderate amount of the collagen fibers was observed in the NaF+resveratrol group (Fig. 3C). In the resveratrol group, there was a little amount of the collagen fibers in the lamina propria (Fig. 3D).

Immunohistochemical detection of tumor necrosis factor α

The examination of TNF-α immune stained sections of the control group revealed a negative cellular cytoplasmic immunoreaction in the epithelium, lamina propria, and the muscle fibers (Fig. 3E). While, in the NaF treated group a strong positive immunoreaction was recorded (Fig. 3F). TNF-α immune stained tongue sections from the NaF+resveratrol group showed a weak immunoreaction in the epithelium and a moderate immunoreaction in the lamina propria and the muscle fibers (Fig. 3G). There was a negative TNF-α immunoreaction in the resveratrol group (Fig. 3H).

Electron microscopic examination

Scanning electron microscopic results

The control group showed numerous elongated filiform papillae with pointed tips, they were oriented in one direction (Fig. 4A). Fungiform papillae were observed among the filiform papillae with taste pore on its surface (Fig. 4B). In the NaF treated group, epithelial exfoliation of the filiform and fungiform papillae was seen. The filiform papillae had flat tips (Fig. 4C, D). There were wide areas of papillary loss and markedly distorted filiform papillae with loss of its elongated appearance and typical features. Some papillae appeared with extensive exfoliations and ulceration (Fig. 4E, F). In the NaF+resveratrol group, numerous filiform papillae with preserved elongated appearance and pointed ends (Fig. 4G), but there was a minor exfoliation in the filiform and fungiform papillae (Fig. 4H). In the resveratrol group, normal numerous elongated filiform papillae with pointed ends were observed. They were oriented in one direction (Fig. 4I). The fungiform papillae were observed among the filiform papillae (Fig. 4J).
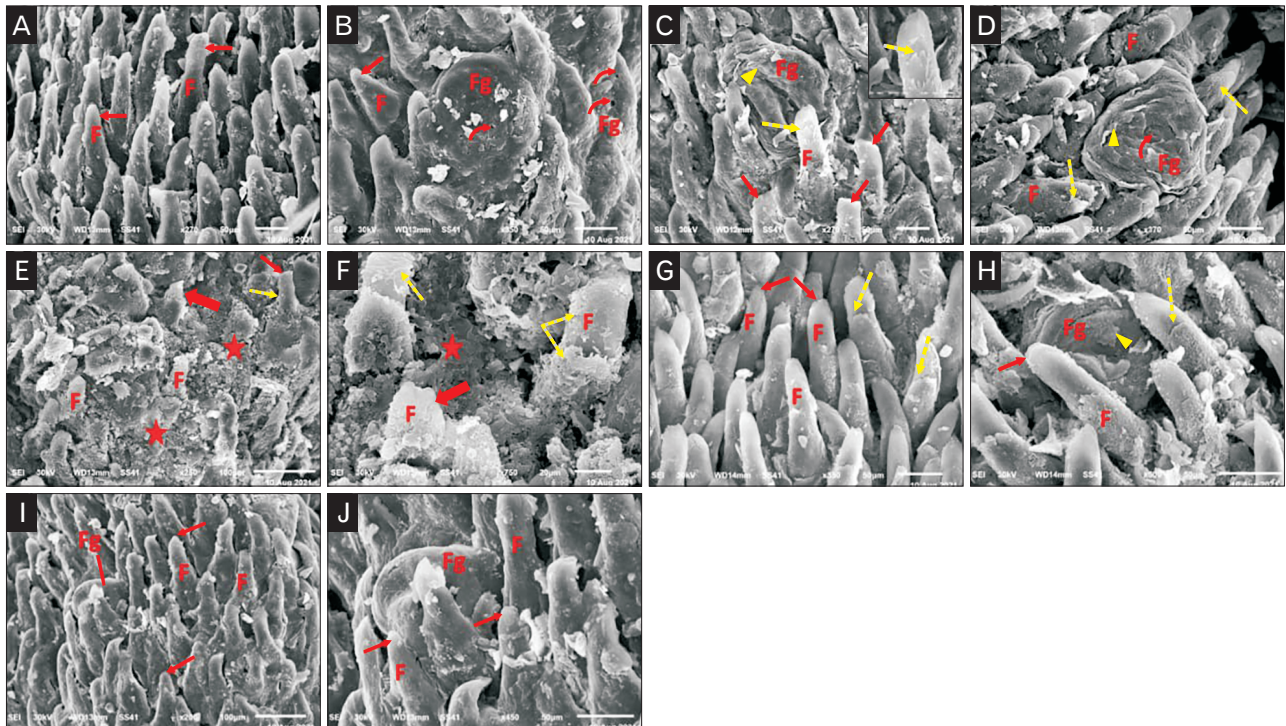
Fig. 4. A scanning electron photomicrograph shows the pathological changes of the albino rat tongue induced by sodium fluoride and their amelioration by resveratrol. The control group (A, B): (A) Numerous elongated filiform papillae (F) with pointed tip (arrow) oriented in one direction (×270, scale bar=50 μm). (B) Fungiform papillae (Fg) are seen among the filiform papillae (F) with a taste pore (curved arrow) on its surface (×350, scale bar=50 μm). NaF treated group (C–F): (C, D) Filiform papillae (F) with flattened tip (arrows) and epithelial exfoliation in the filiform papillae (dotted arrows), clarified also in the inset figure which shows higher magnification view. The fungiform papillae (Fg) with a taste pore (curved arrow) on its surface show epithelial exfoliation (arrowheads) (C: ×270, scale bar=50 μm; the inset figure: ×1,400, scale bar=10 μm; D: ×370, scale bar=50 μm). (E, F) Wide areas of papillary loss (stars) and markedly distorted filiform papillae (F) with loss of its elongated appearance and typical features (thick arrow), other papillae with extensive exfoliations (dotted arrows) with flattened tip (arrow) (E: ×250, scale bar=100 μm; F: ×750, scale bar=20 μm). NaF+resveratrol group (G, H): (G) Filiform papillae (F) with preserved elongated appearance and pointed tips (arrows) and a minor exfoliation (dotted arrow) in the filiform papillae (×350, scale bar=50 μm). (H) Minor epithelial exfoliation (dotted arrow) in the filiform papillae with pointed tip (arrow). The fungiform papillae (Fg) show little epithelial exfoliation (arrowhead) (×500, scale bar=50 μm). Resveratrol group (I, J): The numerous elongated filiform papillae (F) with pointed tips (arrows) oriented in one direction and the fungiform papillae (Fg) were seen among the filiform papillae (I: ×200, scale bar=100 μm; J: ×450, scale bar=50 μm).

Transmission electron microscopic results

The control group showed parallel myofibrils, with well recognized z lines bounding the functional muscle unit (sarcomer). Mitochondria are seen between the myofibrils and below the sarcolemma. Euchromatic oval nucleus was observed (Fig. 5A, B). In the NaF treated group, myofibrils appeared atrophied, widely separated and fragmented. Also, areas of myofibrils loss and poorly observed to absent z lines were recorded. The pyknotic nucleus and congested blood vessel were observed and the mitochondria were small and fragmented (Fig. 5C–E). In the NaF+resveratrol group, there were parallel myofibrils with well recognized z lines and mitochondria between the myofibrils, in addition, euchromatic oval nucleus was seen and some myofibrils appeared atro-phied with little separation. Also, there was still small areas of myofibril loss (Fig. 5F, G). In the resveratrol group, the myofibrils appeared parallel, well recognized z lines, and mitochondria between the myofibrils were observed (Fig. 5H).

Statistical analysis results

Tongue weight
Statistical analysis of the tongue weight showed non significant difference among the 4 groups (P>0.05; Table 1, Fig. 6A).

The area percentage of the collagen fibers& optical density of TNF α
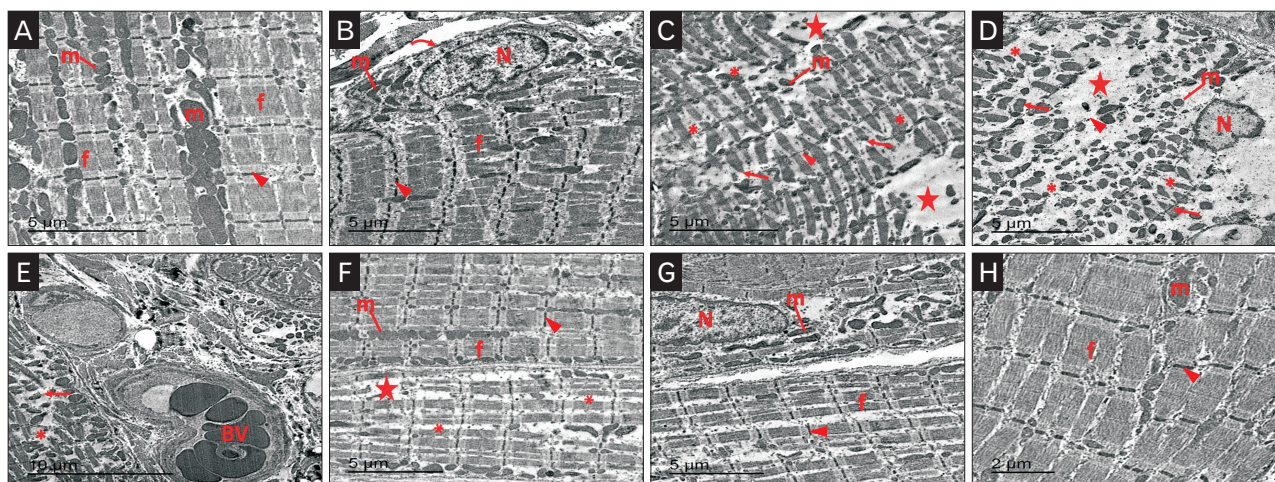Semiquantitative assessment of the AP of the collagen fi-

Fig. 5. A transmission electron photomicrograph shows the pathological changes in the albino rat tongue induced by sodium fluoride and their amelioration by resveratrol. Control group (A, B): (A) Parallel myofibrils (f), well-recognized z lines (arrowhead), and the mitochondria (m) between the myofibrils. (B) Euchromatic oval nucleus (N), mitochondria (m) below the sarcolemma (curved arrow), parallel myofibrils (f), and well-recognized z lines (arrowhead). NaF treated group (C–E): (C) Atrophied, widely separated (*) and fragmented (arrows) myofibrils, areas with myofibrils loss (star), poorly observed to absent z lines (arrowhead), small and fragmented mitochondria (m). (D) Pyknotic nucleus (N), atrophied widely separated (*) and fragmented (arrows) myofibrils, areas with myofibrils loss (star), poorly observed to absent z lines (arrowhead), small and fragmented mitochondria (m). (E) Congested blood vessel (BV), atrophied, widely separated (*), and fragmented myofibrils (arrow). NaF+resveratrol group (F, G): (F) Parallel myofibrils (f), well-recognized z lines (arrowhead), mitochondria (m) between the myofibrils. Some atrophied myofibrils with little separation (*), a small area with myofibrils loss (star). (G) Euchromatic oval nucleus (N), Parallel myofibrils (f), well-recognized z lines (arrowhead), mitochondria (m). (H) Resveratrol group shows parallel myofibrils (f), well recognized z lines (arrowhead), mitochondria (m) between the myofibrils. (A–D, F, G) ×4,000, scale bar=5 μm; (E) ×6,000, scale bar=10 μm; (H) ×10,000, scale bar=2 μm.
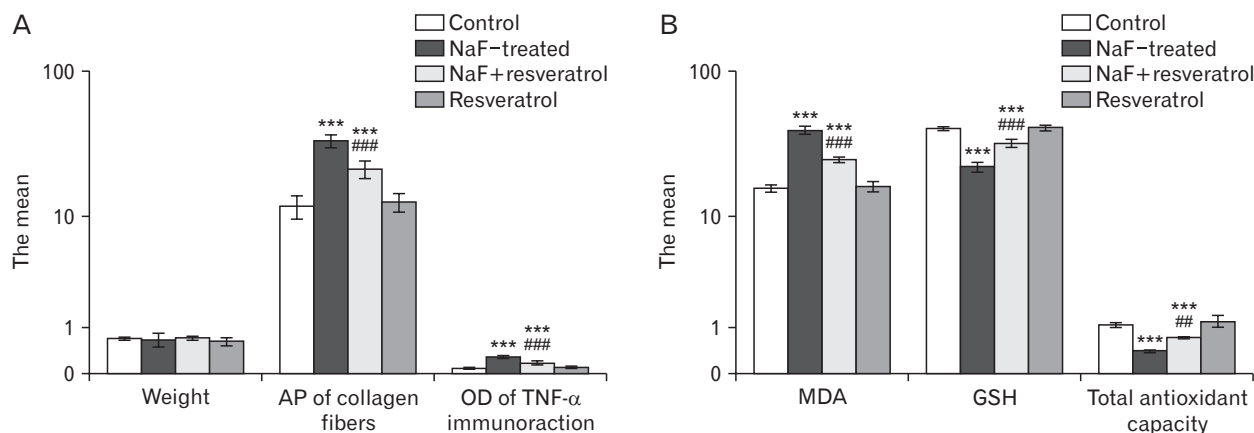

Fig. 6. Bar chart showing (A) Statistical comparison of the tongue weight, area percentage (AP) of the collagen fibers, and the optical density (OD) of tumor necrosis factor α immune-reaction among the 4 groups using one way ANOVA test and least significant difference (LSD) *post-hoc* test. (B) Statistical comparison of the malondialdehyde (MDA), reduced glutathione (GSH), and the total antioxidant capacity tissue levels of the tongue among the 4 groups using one way ANOVA test and LSD *post-hoc* test. Comparison in relation to the control group, ***P<0.001; comparison in relation to the NaF treated group, ##P<0.01, ###P<0.001.

Table 1. Statistical comparison of the tongue weight, the AP of the collagen fibers, and the OD of TNF-α immunoreaction in the tongue

Variable	Control (n=6)	NaF (n=6)	NaF+revasterol (n=6)	Revasterol (n=6)	F	P-value
Weight (g)	0.68±0.04	0.65±0.21	0.70±0.05	0.61±0.12	0.589	>0.05
AP of collagen fibers	11.73±2.70	33.46±4.13[a]	21.40±2.39[a,b]	12.59±2.39	56.12	<0.001
OD of TNF-α immunoreaction	0.07±0.14	0.27±0.03[a]	0.16±0.04[a,b]	0.08±0.24	54.81	<0.001

Values are presented as mean±standard deviation. F, variation between the groups means/variation within the groups; AP, area percentage; OD, optical density; TNF-α, tumor necrosis factor α. Comparison in relation to the control group, [a]P<0.001; Comparison in relation to the NaF treated group, [b]P<0.001.

Table 2. Statistical comparison of the oxidative markers MDA, GSH tissue level, and the total antioxidant capacity of the tongue tissue

Variable	Control (n=6)	NaF (n=6)	NaF+resveratrol (n=6)	Resveratrol (n=6)	F	P-value
MDA (nmol/g tissue)	15.80±1.97	40.16±3.13[a]	25.14±1.35[a,c]	16.34±1.37	194.08	<0.001
GSH (mg/g tissue)	41.08±1.55	22.32±2.18[a]	32.64±2.38[a,c]	41.58±2.48	102.90	<0.001
Total antioxidant capacity (mmol/l)	1.07±0.96	0.39±0.01[a]	0.71±0.03[a,b]	1.19±0.26	40.40	<0.001

Values are presented as mean±standard deviation. F, variation between the groups means/variation within the groups; MDA, malondialdehyde; GSH, reduced glutathione. Comparison in relation to the control group, [a]$P<0.001$; comparison in relation to the NaF treated group, [b]$P<0.01$, [c]$P<0.001$.

bers and the OD of TNF-α immunoreaction mean values in MT-stained and TNF-α immunostained tongue sections displayed a very highly significant statistical difference between the groups ($P<0.001$) by using a one-way ANOVA and LSD *post-hoc* test. The NaF treated group showed a very highly significant increase in the mean values of the AP of the collagen fibers and the OD of TNF-α immunoreaction ($P<0.001$) as compared to the control group. In the NaF+resveratrol group a very highly significant ($P<0.001$) decrase in the AP of the collagen fibers and the OD of TNF-α immunoreaction mean values levels were recorded in relation to the NaF treated group. These mean values were still very highly significant ($P<0.001$) in comparison to the control group.There was a non significant difference between the control and the resveratrol groups ($P>0.05$; Table 1, Fig. 6A).

Oxidative malondialdehyde, reduced glutathione, and the total antioxidant level results

Statistical analysis of the MDA tissue level by Anova test and LSD *post-hoc* test reaveled a significant difference between the 4 groups ($P<0.001$). MDA level showed a significant ($P<0.001$) incraese in the NaF treated group compared to the control and the resveratrol groups. In the NaF+resveratrol group, a significant ($P<0.001$) decrease in MDA level mean values was recorded in relation to the NaF treated group, these mean values were significantly different ($P<0.001$) from the control and the resveratrol groups (Table 2, Fig. 6B).

Statistical analysis of GSH tissue level and the total antioxidant capacity of the tongue tissue homogenate reaveled a significant difference between the 4 groups ($P<0.001$). GSH tissue levels showed a significant ($P<0.001$) decrease in the NaF treated group in comparison to the control and the resveratrol groups. In the NaF+resveratrol group, a significant ($P<0.001$) increase was recorded in the GSH level and the total antioxidant capacity mean values in relation to the NaF treated group, these mean values were significantly different ($P<0.001$) from the control and the resveratrol groups (Table 2, Fig. 6B).

Discussion

The tongue is a muscular organ consists of epithelium, connective tissue, and muscles, with the epithelium thrown into number of lingual papillae and being a mobile organ which has motor functions in eating and speaking [29]. NaF is frequently added in ionic form to drinking water and different foods, where it rapidly passes through the intestinal mucosa and interferes with the living system's major metabolic pathways. Several investigations demonstrated that NaF induced toxicity and pathological effects on the different body organs due to its interaction with the cellular systems. However, none of those studies investigated its toxic effect on the tongue. The present work was undertaken to study the ultrastructural changes which might occur in the tongue tissue of the adult albino rats after the NaF administration. The chosen route was orally to mimic the human exposure. Also, resveratrol was used to evaluate its ability to reduce the NaF induced pathological changes on the tongue. Furthermore, we used male rats only to avoid report of changes due to gender difference [30].

In the current work, a papillary distortion in the form of atrophied filiform papillae with flattened end and distorted fungiform papillae with degenerated taste buds were observed in the NaF treated group. The tongue papillae are of two types, the gustatory papilla which contains taste bud and is responsible for the taste sensation such as fungiform papilla and the mechanical papilla which is involved in friction between the tongue and food substances, so it plays a role in tongue surface protection, mastication, and swallowing [31]. In fact, the long filiform papilla with its pointed end is essential to allow licked soft food into the mouth, such as ice cream, filiform papillae are more developed in rodents than in human [32]. Filiform papillae were considered by Osman et al. [33] to be the earliest papillae to undergo damage and degeneration. The distortion in papillary shape reported in our study would be suggested to affect its functional efficiency. Also, extensive epithelial papillary exfoliation and ulceration were observed in this study by scanning electron

microscopy, it was reported that fluoride toothpaste was associated with oral soft tissue exfoliation and damage [34].

Our results revealed necrotic muscle fibers with pyknotic nuclei and areas of complete loss of the myofibrils and papillae in addition to a state of an oxidative stress. These results explained by Song et al. [35] who found that the NaF decreases the cell viability in a time and dose dependent manner. Moreover, cellular exfoliation has been observed in association with stressful conditions that results in apoptosis and necrosis [36]. Sever cellular exfoliation was recorded to be associated with neoplasm that induces loss of cell adhesion and disruption of normal interactions with underlying stroma related to malignancy progression [37]. However, the NaF was reported to be non-carcinogenic agent [38].

In the current study, the TNF-α immune reaction was excessive in the NaF treated group and showed a very highly significant increase in the mean OD of the inflammatory marker TNF-α (*P*<0.001) in comparison to the control and resveratrol groups. This result was aligned with the study of Lu et al. [39] who hypothesized that the NaF stimulated apoptosis through TNF receptor-1 signaling pathway. TNF-α efficiently mediates inflammatory and immune functions. It is mainly produced by macrophages and monocytes [40].

In our work, a collection of inflammatory cells infiltration was observed in the lamina propria, these results suggest the inflammatory reaction induced by the NaF. Also, excess collagen was observed in the lamina propria of the NaF treated group with the mean AP of the collagen fibers showed a very highly significant difference (*P*<0.001) from the control & resveratrol groups. No excess collagen was observed among the muscle fibers. Fujita et al. [41] reported that overexpression of TNF-α was found to diminish the lung fibrosis in mice.

This study demonstrated multiple small fragmented mitochondria with no swelling in the NaF treated group. The NaF is known to induce a damage in the mitochondrial ultrastructure in conjunction with lipid peroxidation, mitochondrial membrane depolarization, and cellular apoptosis [35, 42]. NaF-induced mitochondrial oxidative stress injuries via decreased Sirtuin 1 protein expression and stimulating acetylation of manganese superoxide dismutase. The mitochondria are under a state of continuous division and fusion forming an interconnecting network which undergoes disintegration during apoptosis. The result is development of numerous and small mitochondria, a process called mitochondrial fragmentation in which the mitochondria lose

their tubular structure with formation of vesicular shapes and are observed in association with oxidative stress [43].

It was found that mitochondrial fusion and fission related proteins have an active role in apoptosis induction [44, 45]. Fragmentation occurs after mitochondrial membrane permeation but itself inhibits membrane permeation later [46]. This can explain the lack of mitochondrial swelling in our study. Swelling of the mitochondria occurs as result of increased membrane permeation; an essential step in the apoptotic cell death [47]. In our study, the statistical analysis of MDA level showed a significant (*P*<0.001) increase in the NaF treated group as compared to the control and resveratrol groups. GSH tissue level and the total antioxidant capacity of the tongue reaveled a significant (*P*<0.001) decrease in the NaF treated group as compared to the control and resveratrol groups. These results are sugesstive of an oxidative stress state and are in accordance with Lu et al. [39] who noticed that the NaF increased reactive oxygen species (ROS) and MDA levels and diminished mRNA expression levels and activities of superoxide dismutase (SOD), GSH, and catalase. The NaF decreased SOD activity by indirect or direct ways, thus triggers generation of ROS which destroys the cell membrane structure [48]. It was stated that factors that affect the expression or activity of SOD leads to diminished antioxidant capacity of the cell [49]. Increased the production of free radicals and decreased the levels of several antioxidant enzymes were considered to be the mechanisms of fluoride induced toxicity as recorded by [50–52]. Oxidative stress reported in this study can explain the NaF pathological effects which observed in the tongue. Regarding muscle necrosis and separation, oxidative stress can affect the cellular signaling pathways involved in regulation of myocyte protein formation and breakdown; in fact, the increased ROS increase the muscle proteolysis and inhibit the protein formation [53]. Also, with regard to inflammation, ROS activates proinflammatory genes through regulation of several transcription factors and kinases [54]. ROS generation was accused to be the cause of inflammatory cell infiltration as mentioned by [55].

The current work revealed that the NaF showed no effect on the body weight with insignificant difference in the weight mean values among the studied groups. This result is contradicted by Amaral et al. [56] who reported a decrease in the body weight in rats subjected to the NaF in drinking water. While Vohra [57] reported no change in the weight of Japanese quail subjected to a similar dose of NaF.

The histological examination of the NaF+resveratrol group revealed marked preservations of the normal structure of the filiform and the fungiform papillae, and the tongue muscle fibers. These observations matched with the previous studies of [58, 59] who mentioned that histopathological alterations induced by fluoride were not observed in the liver and brain of the rats received resveratrol. In the same group (NaF+resveratrol), a significant ($P<0.001$) increase of both GSH tissue level and the total antioxidant capacity and a significant decrease ($P<0.001$) in MDA was recorded in relation to the NaF treated group. Our results suggested that resveratrol is a strong antioxidant against the oxidative stress caused by the NaF in the tongue. Resveratrol is known to prevent over production of ROS and provides protection for cells against oxidative stress [60]. The antioxidant effect of resveratrol is produced through its ability to scavenge free radicals and by the modulation of the antioxidative pathways. It has the ability to stimulate the activities of variable antioxidant enzymes [61, 62]. Furthermore, resveratrol has a high hydrophilic and lipophilic content, which contributes to its effectiveness when compared to the other antioxidants such as vitamins E and C [63]. When compared to the control group, the resveratrol group showed no statistically significant changes in the oxidative stress parameters. These results support resveratrol as a protective agent [59, 64].

The immune-expression of TNF-α in the NaF+resveratrol group showed a siginificant decrsease in the OD in comparison to the NaF treated group. This revealed an anti infilammatory effect of resveratrol. Resveratrol was reported to induce its anti inflammatory effect through inhibition of the cyclooxygenase enzyme [65]. Also, it can decraese the secretion and the expression of the inflammatory factors and prevent inflammation through inhibition of nuclear factor kappa B, TNFα and interleukin-6 serum levels [66].

The ant-inflammatory and antioxidant properties and many other effects of resveratrol are mediated through activation of Sirtuin 1. A mechanism seems to antagonize that of the NaF which suggest resveratrol as ideal to protect against NaF effects [67].

Besides, the NaF+resveratrol group revealed a significant improvement of the collagen surface area in MT-stained sections as compared with the NaF treated group. The resveratrol emaciated the tongue fibrosis induced by the NaF via decreasing the collagen deposition. This finding might be in accordance with [68, 69] who reported that resveratrol prevented the liver fibrosis and the pulmonary fibrosis by molecular mechanisms.

In the current study, the NaF+ resveratrol group revealed improvement of the mitochondrial shape as compared with the NaF treated group which showed the small fragmented mitochondria. Resveratrol stimulates the mitochondrial fusion with resultant development of a large mitochondrial network [70]. Resveratrol can enhance the synthesis of the cellular mitochondria and stimulates the proliferative activated receptor-γ coactivator 1α promoting the mitochondrial function and number to decrease the cell damage induced by toxins [71]. Also, the studies [68, 72] recorded that resveratrol improved the mitochondrial function by increasing membrane potential.

In conclusion, NaF causes histopathological alterations in the tongue of the adult albino rats through the oxidative stress. It is recommended for resveratrol intake to relieve the NaF injury by modulating the inflammatory promarker TNF-α and decreasing the collagen deposition in the tongue. More studies in the future may be needed to reveal more mechanisms by which NaF led to tongue injury.

ORCID

Emtethal M. El-Bestawy:
https://orcid.org/0000-0002-1065-8848
Asmaa M. Tolba: https://orcid.org/0000-0002-8347-9007
Walaa A. Rashad: https://orcid.org/0000-0001-7291-3798

Author Contributions

Conceptualization: EMEB. Data acquisition: AMT. Data analysis or interpretation: AMT. Drafting of the manuscript: WAR. Critical revision of the manuscript: EMEB, AMT, WAR. Approval of the final version of the manuscript: all authors.

Conflicts of Interest

No potential conflict of interest relevant to this article was reported.

Acknowledgements

References

1. Gao J, Tian X, Yan X, Wang Y, Wei J, Wang X, Yan X, Song G. Selenium exerts protective effects against fluoride-induced apoptosis and oxidative stress and altered the expression of Bcl-2/caspase family. Biol Trace Elem Res 2021;199:682-92.

2. Abed KF, Alwakeel SS. Mineral and microbial contents of bottled and tap water in Riyadh, Saudi Arabia. Middle East J Sci Res 2007;2:151-6.

3. Pendrys DG. Fluoride ingestion and oral health. Nutrition 2001;17:979-80.

4. Al-hayani A, Elshal EB, Aal IHA, Al-Shammeri E. Does vitamin E protect against sodium fluoride toxicity on the cerebellar cortex of albino rats? Middle East J Sci Res 2013;16:1019-26.

5. Fung KF, Zhang ZQ, Wong JWC, Wong MH. Fluoride contents in tea and soil from tea plantations and the release of fluoride into tea liquor during infusion. Environ Pollut 1999;104:197-205.

6. Jacinto-Alemán LF, Hernández-Guerrero JC, Trejo-Solís C, Jiménez-Farfán MD, Fernández-Presas AM. In vitro effect of sodium fluoride on antioxidative enzymes and apoptosis during murine odontogenesis. J Oral Pathol Med 2010;39:709-14.

7. Rahmani S, Rezaei M. Toxicity of fluoride on isolated rat liver mitochondria. J Fluor Chem 2020;239:109636.

8. O'Neil MJ, Smith A, Heckelman PE, Budavari S. The Merck index: an encyclopedia of chemicals, drugs, and biologicals. 13th ed. Whitehouse Station: Merck; 2001.

9. Ahmed SK, Kalleny NK, El Moneim Attia AA, Elkateb LA. The possible protective role of chromium chloride against sodium fluoride-induced changes in the structure of the cerebellar cortex of the adult male albino rat. Egypt J Histol 2015;38:402-14.

10. Mondal K, Nath S. Fluoride contamination on aquatic organisms and human body at Purulia and Bankura district of West Bengal, India. Bull Environ Pharmacol Life Sci 2015;4:112-4.

11. Dhar V, Bhatnagar M. Physiology and toxicity of fluoride. Indian J Dent Res 2009;20:350-5.

12. Yan X, Yang X, Hao X, Ren Q, Gao J, Wang Y, Chang N, Qiu Y, Song G. Sodium fluoride induces apoptosis in H9c2 cardiomyocytes by altering mitochondrial membrane potential and intracellular ROS level. Biol Trace Elem Res 2015;166:210-5.

13. Al Badawi MH, Mahmoud OM, Salem NA. Therapeutic potential of omega-3 against sodium fluoride toxicity on the cerebellar cortex of adult male albino rats. Egypt J Histol 2016;39:170-8.

14. Basha MP, Begum S, Madhusudhan N. Antioxidants in the management of fluoride induced neural oxidative stress in developing rats. Int J Pharm Sci Res 2014;5:201-6.

15. El-Khair DMA, El-Safti FENA, El-Habeby MM, El-Kholy WB, El-Sherif NM. Effect of sodium fluoride on the grey matter of spinal cord in the albino rat and the protective role of green tea extract. Anatomy 2016;10:114-33.

16. Kanagaraj VV, Panneerselvam L, Govindarajan V, Ameeramja J, Perumal E. Caffeic acid, a phyto polyphenol mitigates fluoride induced hepatotoxicity in rats: a possible mechanism. Biofactors 2015;41:90-100.

17. Shivarajashankara Y, Shivashankara A, Bhat PG, Rao SH. Effect of fluoride intoxication on lipid peroxidation and antioxidant systems in rats. Fluoride 2001;34:108-13.

18. Oliveira BV, Barros Silva PG, Nojosa Jde S, Brizeno LA, Ferreira JM, Sousa FB, Mota MR, Alves AP. TNF-alpha expression, evaluation of collagen, and TUNEL of Matricaria recutita L. extract and triamcinolone on oral ulcer in diabetic rats. J Appl Oral Sci 2016;24:278-90.

19. Chamani G, Zarei MR, Mehrabani M, Mehdavinezhad A, Vahabian M, Ahmadi-Motamayel F. Evaluation of honey as a topical therapy for intraoral wound healing in rats. Wounds 2017;29:80-6.

20. Al-Ayed MS, Asaad AM, Qureshi MA, Attia HG, AlMarrani AH. Antibacterial activity of Salvadora persica L. (Miswak) extracts against multidrug resistant bacterial clinical isolates. Evid Based Complement Alternat Med 2016;2016:7083964.

21. Nalagoni CSR, Karnati PR. Protective effect of resveratrol against neuronal damage through oxidative stress in cerebral hemisphere of aluminum and fluoride treated rats. Interdiscip Toxicol 2016;9:78-82.

22. Zeng XX, Deng J, Xiang J, Dong YT, Cao K, Liu XH, Chen D, Ran LY, Yang Y, Guan ZZ. Resveratrol attenuated the increased level of oxidative stress in the brains and the deficit of learning and memory of rats with chronic fluorosis. Fluoride 2019;52:149-60.

23. Agustina F, Sofro ZM, Partadiredja G. Subchronic administration of high-dose sodium fluoride causes deficits in cerebellar Purkinje cells but not motor coordination of rats. Biol Trace Elem Res 2019;188:424-33.

24. Sharma C, Suhalka P, Bhatnagar M. Curcumin and resveratrol rescue cortical-hippocampal system from chronic fluoride-induced neurodegeneration and enhance memory retrieval. Int J Neurosci 2018;128:1007-21.

25. Suvarna SK, Layton C, Bancroft JD. Bancroft's theory and practice of histological techniques. 7th ed. Philadelphia: Churchill Livingstone; 2013. p. 173-214.

26. Rau E, Gostev A, Shiqiu Z, Phang D, Chan D, Thong D, Wong W. Comparative analysis of scanning electron microscopy techniques for semiconductors: electron-beam-induced potential method, single-contact electron-beam-induced current method, and thermoacoustic detection. Russ Microelectron 2001;30:207-18.

27. Ayache J, Beaunier L, Boumendil J, Ehret G, Laub D. Sample preparation handbook for transmission electron microscopy techniques. New York: Springer; 2010.

28. Erel O. A novel automated direct measurement method for total antioxidant capacity using a new generation, more stable ABTS radical cation. Clin Biochem 2004;37:277-85.

29. Mistretta CM, Bradley RM. The fungiform papilla is a complex, multimodal, oral sensory organ. Curr Opin Physiol 2021;20:165-73.

30. Hsu PC, Wu HK, Huang YC, Chang HH, Chen YP, Chiang JY, Lo LC. Gender- and age-dependent tongue features

in a community-based population. Medicine (Baltimore) 2019;98:e18350.

31. Abayomi TA, Ofusori DA, Ayoka OA, Odukoya SA, Omotoso EO, Amegor FO, Ajayi SA, Ojo GB, Oluwayinka OP. A comparative histological study of the tongue of rat (Rattus norvegicus), bat (Eidolon Helvum) and pangolin (Manis tricuspis). Int J Morphol 2009;27:1111-9.

32. Maynard RL, Downes N. Alimentary canal or gastrointestinal tract. In: Maynard RL, Downes N, editors. Anatomy and Histology of the Laboratory Rat in Toxicology and Biomedical Research. London: Academic Press; 2019. p.147-58.

33. Osman HI, Abd El Razek N, Koura SA. Histological changes of rat lingual papillae due to chromium toxicity and the protective role of vitamin E. Egypt Dent J 2006;52:193-200.

34. Yang M, Zhao HP, Yang J. [Effect of toothpaste containing emulsifier 30 and sodium lauryl sulfate surfactant on the integrity of oral epithelium]. Shanghai Kou Qiang Yi Xue 2021;30:312-5. Chinese.

35. Song C, Fu B, Zhang J, Zhao J, Yuan M, Peng W, Zhang Y, Wu H. Sodium fluoride induces nephrotoxicity via oxidative stress-regulated mitochondrial SIRT3 signaling pathway. Sci Rep 2017;7:672. Erratum in: Sci Rep 2018;8:7737.

36. Kaeffer B. Exfoliated epithelial cells: potentials to explore gastrointestinal maturation of preterm infants. Rev Bras Saude Matern Infant 2010;10:13-24.

37. Schwab M. Encyclopedia of Cancer. Berlin: Springer-Verlag; 2011.

38. Maurer JK, Cheng MC, Boysen BG, Anderson RL. Two-year carcinogenicity study of sodium fluoride in rats. J Natl Cancer Inst 1990;82:1118-26.

39. Lu Y, Luo Q, Cui H, Deng H, Kuang P, Liu H, Fang J, Zuo Z, Deng J, Li Y, Wang X, Zhao L. Sodium fluoride causes oxidative stress and apoptosis in the mouse liver. Aging (Albany NY) 2017;9:1623-39.

40. Aronson JK. Tumor necrosis factor alfa. In: Aronson JK, editor. Meyler's Side Effects of Drugs. 16th ed. Amsterdam: Elsevier; 2016. p.230-32.

41. Fujita M, Shannon JM, Morikawa O, Gauldie J, Hara N, Mason RJ. Overexpression of tumor necrosis factor-alpha diminishes pulmonary fibrosis induced by bleomycin or transforming growth factor-beta. Am J Respir Cell Mol Biol 2003;29:669-76.

42. Adkins EA, Brunst KJ. Impacts of fluoride neurotoxicity and mitochondrial dysfunction on cognition and mental health: a literature review. Int J Environ Res Public Health 2021;18:12884.

43. Peng W, Xu S, Zhang J, Zhang Y. Vitamin C attenuates sodium fluoride-induced mitochondrial oxidative stress and apoptosis via Sirt1-SOD2 pathway in F9 cells. Biol Trace Elem Res 2019;191:189-98.

44. Suen DF, Norris KL, Youle RJ. Mitochondrial dynamics and apoptosis. Genes Dev 2008;22:1577-90.

45. Miyazono Y, Hirashima S, Ishihara N, Kusukawa J, Nakamura KI, Ohta K. Uncoupled mitochondria quickly shorten along their long axis to form indented spheroids, instead of rings, in a

46. Arnoult D. Mitochondrial fragmentation in apoptosis. Trends Cell Biol 2007;17:6-12.

47. Davis MA, Jeffery EH. Organelle biochemistry and regulation of cell death. In: Haschek WM, Rousseaux CG, Wallig MA, editors. Handbook of Toxicologic Pathology. 2nd ed. Orlando: Academic Press; 2002. p.67-81.

48. Mittal M, Flora SJ. Effects of individual and combined exposure to sodium arsenite and sodium fluoride on tissue oxidative stress, arsenic and fluoride levels in male mice. Chem Biol Interact 2006;162:128-39.

49. Holley AK, Bakthavatchalu V, Velez-Roman JM, St Clair DK. Manganese superoxide dismutase: guardian of the powerhouse. Int J Mol Sci 2011;12:7114-62.

50. Hassan HA, Abdel-Aziz AF. Evaluation of free radical-scavenging and anti-oxidant properties of black berry against fluoride toxicity in rats. Food Chem Toxicol 2010;48:1999-2004.

51. Nabavi SM, Nabavi SF, Eslami S, Moghaddam AH. In vivo protective effects of quercetin against sodium fluoride-induced oxidative stress in the hepatic tissue. Food Chem 2012;132:931-5.

52. Panneerselvam L, Subbiah K, Arumugam A, Senapathy JG. Ferulic acid modulates fluoride-induced oxidative hepatotoxicity in male Wistar rats. Biol Trace Elem Res 2013;151:85-91.

53. Powers SK, Smuder AJ, Judge AR. Oxidative stress and disuse muscle atrophy: cause or consequence? Curr Opin Clin Nutr Metab Care 2012;15:240-5.

54. Ranneh Y, Ali F, Akim AM, Hamid HA, Khazaai H, Fadel A. Crosstalk between reactive oxygen species and pro-inflammatory markers in developing various chronic diseases: a review. Appl Biol Chem 2017;60:327-38.

55. Johar D, Roth JC, Bay GH, Walker JN, Kroczak TJ, Los M. Inflammatory response, reactive oxygen species, programmed (necrotic-like and apoptotic) cell death and cancer. Rocz Akad Med Bialymst 2004;49:31-9.

56. Amaral SL, Azevedo LB, Buzalaf MAR, Fabricio MF, Fernandes MS, Valentine RA, Maguire A, Zohoori FV. Effect of chronic exercise on fluoride metabolism in fluorosis-susceptible mice exposed to high fluoride. Sci Rep 2018;8:3211.

57. Vohra P. Fluoride tolerance of Japanese quail. Poult Sci 1973;52:391-3.

58. Tunali-Akbay T, Sehirli O, Ercan F, Sener G. Resveratrol protects against methotrexate-induced hepatic injury in rats. J Pharm Pharm Sci 2010;13:303-10.

59. Atmaca N, Atmaca HT, Kanici A, Anteplioglu T. Protective effect of resveratrol on sodium fluoride-induced oxidative stress, hepatotoxicity and neurotoxicity in rats. Food Chem Toxicol 2014;70:191-7.

60. Pignet AL, Schellnegger M, Hecker A, Kohlhauser M, Kotzbeck P, Kamolz LP. Resveratrol-induced signal transduction in wound healing. Int J Mol Sci 2021;22:12614.

61. Alarcon de la Lastra C, Villegas I, Martin AR. Resveratrol as an Antioxidant. In: Aggarwal BB, Shishodia S, editors. Resveratrol in Health and Disease. Boca Raton: CRC Press; 2006. p.33-56.

62. Konyalioglu S, Armagan G, Yalcin A, Atalayin C, Dagci T. Effects of resveratrol on hydrogen peroxide-induced oxidative stress in embryonic neural stem cells. Neural Regen Res 2013;8:485-95.

63. Kasdallah-Grissa A, Mornagui B, Aouani E, Hammami M, El May M, Gharbi N, Kamoun A, El-Fazaâ S. Resveratrol, a red wine polyphenol, attenuates ethanol-induced oxidative stress in rat liver. Life Sci 2007;80:1033-9.

64. Kolouchova-Hanzlikova I, Melzoch K, Filip V, Smidrkal J. Rapid method for resveratrol determination by HPLC with electrochemical and UV detections in wines. Food Chem 2004;87:151-8.

65. Kong F, Zhang R, Zhao X, Zheng G, Wang Z, Wang P. Resveratrol raises *in vitro* anticancer effects of paclitaxel in NSCLC cell line A549 through COX-2 expression. Korean J Physiol Pharmacol 2017;21:465-74.

66. Zhou ZX, Mou SF, Chen XQ, Gong LL, Ge WS. Anti-inflammatory activity of resveratrol prevents inflammation by inhibiting NF-κB in animal models of acute pharyngitis. Mol Med Rep 2018;17:1269-74.

67. Duntas LH. Resveratrol and its impact on aging and thyroid function. J Endocrinol Invest 2011;34:788-92.

68. Chen TT, Peng S, Wang Y, Hu Y, Shen Y, Xu Y, Yin J, Liu C, Cao J. Improvement of mitochondrial activity and fibrosis by resveratrol treatment in mice with *Schistosoma japonicum* infection. Biomolecules 2019;9:658.

69. Wang J, He F, Chen L, Li Q, Jin S, Zheng H, Lin J, Zhang H, Ma S, Mei J, Yu J. Resveratrol inhibits pulmonary fibrosis by regulating miR-21 through MAPK/AP-1 pathways. Biomed Pharmacother 2018;105:37-44.

70. Robb EL, Moradi F, Maddalena LA, Valente AJF, Fonseca J, Stuart JA. Resveratrol stimulates mitochondrial fusion by a mechanism requiring mitofusin-2. Biochem Biophys Res Commun 2017;485:249-54.

71. Lagouge M, Argmann C, Gerhart-Hines Z, Meziane H, Lerin C, Daussin F, Messadeq N, Milne J, Lambert P, Elliott P, Geny B, Laakso M, Puigserver P, Auwerx J. Resveratrol improves mitochondrial function and protects against metabolic disease by activating SIRT1 and PGC-1alpha. Cell 2006;127:1109-22.

72. Abolaji AO, Ajala VO, Adigun JO, Adedara IA, Kinyi HW, Farombi EO. Protective role of resveratrol, a natural polyphenol, in sodium fluoride-induced toxicity in *Drosophila melanogaster*. Exp Biol Med (Maywood) 2019;244:1688-94.